



Published in final edited form as:

*Oncogene*. 2017 September 14; 36(37): 5309–5320. doi:10.1038/onc.2016.261.

## A Novel Interaction of PAK4 with PPAR $\gamma$ to Regulate Nox1 and Radiation-Induced Epithelial-to-Mesenchymal Transition in Glioma

Divya Kesanakurti<sup>1</sup>, Dilip Maddirela<sup>3</sup>, Sanjeeva Mohanam<sup>3</sup>, Balveen Kaur<sup>2</sup>, and Vinay K. Puduvalli<sup>1</sup>

<sup>1</sup>Division of Neuro-oncology, The Dardinger Center for Neuro-oncology and Neurosciences, The Ohio State University Comprehensive Cancer Center, Columbus, OH 43210, USA

<sup>2</sup>Department of Neurosurgery, The Dardinger Center for Neuro-oncology and Neurosciences, The Ohio State University Comprehensive Cancer Center, Columbus, OH 43210, USA

<sup>3</sup>Department of Cancer Biology and Pharmacology, University of Illinois College of Medicine at Peoria, Peoria, IL 61605, USA

### Abstract

Tumor recurrence in glioblastoma (GBM) is, in part, attributed to increased epithelial-to-mesenchymal transition (EMT) and enhanced tumor cell dissemination in adjacent brain parenchyma after ionizing radiation (IR). EMT is associated with aggressive behavior, increased stem-like characteristics and treatment resistance in malignancies; however, the underlying signaling mechanisms that regulate EMT are poorly understood. We identified grade-dependent PAK4 upregulation in gliomas and further determined its role in mesenchymal transition and radioresistance. IR treatment significantly elevated expression and nuclear localization of PAK4 in correlation with induction of reactive oxygen species (ROS) and mesenchymal transition in GBM cells. Stable PAK4 overexpression promoted mesenchymal transition by elevating EMT marker expression in these cells. Of note, transcription factor-DNA binding arrays and chromatin immunoprecipitation experiments identified the formation of a novel nuclear PAK4/PPAR $\gamma$  complex which was recruited to the promoter of Nox1, a PPAR $\gamma$  target gene. In addition, IR further elevated PAK4/PPAR $\gamma$  complex co-recruitment to Nox1 promoter, and increased Nox1 expression and ROS levels associated with mesenchymal transition in these cells. Conversely, specific PAK4 downregulation decreased PPAR $\gamma$ -mediated Nox1 expression and suppressed EMT in IR-treated cells. *In vivo* orthotopic tumor experiments showed inhibition of growth and suppression of IR-induced PPAR $\gamma$  and Nox1 expression by PAK4 downregulation in tumors. Our results provide the first evidence of a novel role for PAK4 in IR-induced EMT and suggest potential therapeutic efficacy of targeting PAK4 to overcome radioresistance in gliomas.

Users may view, print, copy, and download text and data-mine the content in such documents, for the purposes of academic research, subject always to the full Conditions of use:[http://www.nature.com/authors/editorial\\_policies/license.html#terms](http://www.nature.com/authors/editorial_policies/license.html#terms)

Corresponding authors: Vinay K. Puduvalli, MD and Divya Kesanakurti, PhD, Division of Neuro-oncology, 320 W 10<sup>th</sup> Avenue Starling Loving Hall Suite M410, The Ohio State University Comprehensive Cancer Center, Columbus OH 43210, Phone: 614-688-7592; Fax: 614-366-5763, Vinay.Puduvalli@osumc.edu or Divya.Kesanakurti@osumc.edu.

### Conflict of interest Statement

The authors have no conflict of interest to declare.

## Keywords

Epithelial-to-mesenchymal transition (EMT); Nox1; PAK4; PPAR $\gamma$ ; Radioresistance; Reactive oxygen species (ROS)

---

## Introduction

Epithelial–mesenchymal transition (EMT) is a developmental trans-differentiation program that facilitates the formation of highly motile cells with stem cell capabilities.<sup>14, 68</sup> Cancer cells utilize EMT as an adaptive mechanism to acquire invasive potential which in turn leads to increased metastatic potential and treatment resistance contributing to cancer related deaths.<sup>30, 56</sup> Glioblastoma (GBM) is a lethal primary brain tumor associated with a median survival of ~16 months despite the use of resection, subsequent radiation and chemotherapy.<sup>55, 58</sup> The emerging role of EMT in radioresistance is of particular relevance to GBMs which inevitably recur after initial chemoradiation therapy and targeting signaling pathways that drive acquisition of mesenchymal characteristics could hence be a promising strategy to improve tumor response to treatment and survival.<sup>39, 42</sup> However, mediators of EMT that drive treatment resistance are not well characterized.

The p21-activated kinases (PAKs) are a family of serine/threonine kinases involved in embryonic development, cytoskeletal remodeling, cell motility and proliferation.<sup>15, 51</sup> PAK4 belongs to group II PAKs and is an effector of the Rho GTPase Cdc42 that regulates filopodia formation and anchorage independent growth in cells.<sup>36, 46, 50, 67</sup> Recently accumulating evidences suggest a potential nuclear role for PAK4 in the transcriptional regulation by associating with the ribonucleoprotein complexes through its N-terminal interaction domain<sup>4, 22, 35</sup>. Aberrant expression of PAK4 has been demonstrated by our group and others in several tumors including GBMs and was shown to promote proliferation and invasion of cancer cells.<sup>25, 38, 44, 57, 63</sup> PAK4 expression has been correlated with increasing pathological grade in human cancers which when combined with its key role in driving several aspects of tumor biology suggests that PAK4 is a highly relevant therapeutic target in cancer.

Our preliminary experiments with protein-TF interaction array showed peroxisome proliferator-activated receptor gamma (PPAR $\gamma$ ) as a potential partner for nuclear-PAK4. PPAR $\gamma$  is a member of nuclear-hormone-receptor family transcription factors (TF) which regulate several genes involved in insulin sensitivity, adipocyte differentiation and tumor progression.<sup>11, 16, 34, 43, 48, 62</sup> Stimulus-activated PPAR $\gamma$  heterodimerizes with coactivator retinoid receptor protein (RXR) in the nucleus and interacts with peroxisome-proliferator response element (PPRE) in the promoter of target genes involved in various physiological functions in cells.<sup>11, 34</sup> PPAR $\gamma$  antagonists inhibit proliferation and alter reactive oxygen species (ROS) and stem cell expression in gliomas.<sup>48</sup> Such ROS regulation is mediated in part by NADPH oxidase 1 (Nox1), a member of Nox family of proteins that catalyze the electron transfer from NAD(P)H to molecular oxygen to generate superoxide or hydrogen peroxide.<sup>28</sup> Nox1 overexpression has been implicated in sustained ROS generation which then leads to oncogenic transformation, EMT and aggressive tumor metastases.<sup>47</sup> These data

suggest a possible role for PPAR $\gamma$ -Nox1-ROS axis in EMT and based on these data and our preliminary results, we hypothesized that PAK4 could potentially regulate this axis and modulate EMT and radiation resistance in gliomas.

In this study, we aimed to characterize the role of nuclear-PAK4 in radiation-induced EMT and to determine whether PAK4 can cooperate with PPAR $\gamma$  to regulate downstream targets relevant to ROS regulation such as Nox1 to effect mesenchymal transition of glioma cells.

## Results

### PAK4 promotes mesenchymal transition in glioma cells

Our previous findings showed that PAK4 promotes proliferation and invasion in glioma cells<sup>25</sup>. EMT is implicated in increased tumor invasiveness and metastases. Here, we hypothesize that PAK4 may be potentially involved in mesenchymal transition in gliomas. To test this hypothesis, we examined the effect of PAK4 overexpression and knockdown on EMT in gliomas. Glioma xenograft cells, 4910 and 5310 transfected with full-length human PAK4 (PAK4-FL) (Figure 1A) showed a more spindle shaped morphology when compared to empty vector (EV)-controls (Figure 1B). PAK4-overexpressing cells also showed decreased expression levels of epithelial markers E-cadherin and Zo-1, and increased mesenchymal markers, N-cadherin, vimentin and Slug (Figure 1C). Further, confocal studies confirmed decrease in E-cadherin levels and increased N-cadherin levels in PAK4-FL-treated cells compared to EV-controls (Supplementary Figure S1A). Overexpression of kinase-dead PAK4 mutant (PAK4-K350M) also increased N-cadherin and decreased E-cadherin levels, which suggest that PAK4 regulates mesenchymal transition in glioma cells may follow a kinase-independent mechanism (Supplementary Figure S1B).

Conversely, glioma cells treated with PAK4sh showed a significant reduction (48 hours, ~68%) in PAK4 levels compared with untreated or SV-treated controls (Figure 1D). Morphological studies showed a lack of EMT phenotype in PAK4-knockdown cells which showed decreased spindle shaped morphology when compared to controls (Figure 1E). Moreover, immunoblotting showed increased E-cadherin and Zo-1, and inhibited N-cadherin, vimentin and Slug levels in PAK4sh-treated cells compared to control counterparts (Figure 1D). Further, confocal microscopy showed an increase in E-cadherin and an increase in N-cadherin expression in PAK4sh-treated cells compared to untreated or SV-treated controls (Figure 1F). To further evaluate the effects of PAK4 on cytoskeletal modifications related to EMT, we examined actin stress fiber formation, a feature of EMT, using phalloidin staining in glioma cells in the setting of PAK4-knockdown or -overexpression. PAK4sh-treated cells demonstrated a reduction in stress fiber formation suggesting inhibition of the EMT whereas PAK4-FL cells showed characteristic cytoskeletal remodeling of actin into stress fibers (Supplementary Figure S1C). Together, these data suggest a potent role for PAK4 in the acquisition of mesenchymal phenotype in gliomas.

## IR treatment induces EMT in glioma cells associated with increased PAK4 nuclear translocation and elevated ROS

Nuclear fractionation and immunoblotting experiments revealed nuclear expression of PAK4 in surgical GBM tumor samples (Supplementary Figure S2A) and in GBM cell lines (Supplementary Figure S2B). Further, immunohistochemical analysis using glioma tissue microarray indicated a progressive increase in PAK4 nuclear positivity corresponding with increasing pathological grades of glioma (Supplementary Figure S2C, S2D). Given our results suggesting a role for PAK4 in EMT induction, we examined changes in PAK4 sub-cellular localization and its role in EMT after radiation in glioma cells. 4910 and 5310 cells were treated with IR (8 Gy) and PAK4 expression was examined. IR elevated PAK4 transcriptional (Figure 2A) and protein levels (Figure 2B). Sub-cellular fractionation experiments indicated a significant IR-induced increase in PAK4 nuclear localization in these cells (Figure 2C). Immunocytochemistry confirmed the PAK4 nuclear localization in IR-treated cells, whereas, control cells displayed predominant cytoplasmic localization with very low nuclear expression (Figure 2D). Further, we observed strong EMT-associated morphological changes in IR-treated cells by relative loss of cell-to-cell contacts and acquisition of spindle-like mesenchymal phenotype when compared to untreated controls (Figure 2E). Immunoblotting confirmed IR-induced upregulation of EMT markers N-cadherin, vimentin and Slug and downregulation of E-cadherin and Zo-1 levels (Figure 2F). In line with these results, immunocytochemistry revealed loss of E-cadherin and elevation in N-cadherin levels in IR-treated cells (Figure 2G). Moreover, we observed increased cellular ROS levels 24 hours after IR-treatment in these cells (Figure 2H). These findings indicate an association of IR-induced EMT and ROS upregulation with increased nuclear-PAK4 levels, and suggest a possible role of nuclear-PAK4 in the regulation of IR-induced EMT in glioma.

## Nuclear-PAK4 associates with the nuclear receptor PPAR $\gamma$ in glioma

PAK4 possesses nuclear localization sequence (NLS) and was suggested to facilitate nuclear import of  $\beta$ -catenin and associate with TCF/LEF consensus elements<sup>36</sup>. Based on these previous studies that showed PAK4 association with transcriptional activity<sup>4, 36</sup> and our current results that showed IR-induced EMT and PAK4 nuclear translocation, we further investigated a potential role for nuclear-PAK4 in the IR-induced gene activation through its association with TFs and their consensus elements. Using immunoprecipitated PAK4 from nuclear extracts as bait, we searched for its potential interacting TFs in the nucleus by using immobilized TF-TF interaction arrays. Nuclear-PAK4 immunoprecipitated from untreated-controls showed potential association of PAK4 with GATA, HNF-4, TCF/LEF, PPAR $\alpha$  & PPAR $\gamma$  TFs (Figure 3A), whereas, non-specific IgG showed no obvious binding signal on the array (Supplementary Figure S3A). After IR-treatment, we identified binding of nuclear-PAK4 to several TFs (Figure 3A). Of note, we observed high levels of IR-induced PAK4 association with PPAR $\gamma$ , which is not only implicated in the regulation of several target genes involved in cancer but is also known to have a potential role in EMT.

To further examine the PAK4 and PPAR $\gamma$  interaction, we performed immunoprecipitation (IP) experiments by overexpression of PAK4 (PAK4-FL) or tagged PPAR $\gamma$  (FLAG-PPAR $\gamma$ ) and immunoblotting confirmed the specific binding of PAK4 with PPAR $\gamma$  in glioma cells (Figure 3B and 3C). In order to examine whether the PAK4 kinase activity is required for its

nuclear localization, we performed IPs with EV- and PAK4-K350M-treated 4910 nuclear extracts. Similar to PAK4-FL, kinase-dead PAK4-K350M overexpression elevated PAK4 nuclear expression and subsequently increased binding with PPAR $\gamma$  in these cells (Supplementary Figure S3B). These findings were further confirmed by IP of the endogenous proteins which showed robust interaction between PAK4 and PPAR $\gamma$  in these cells (Figure 3D). GST pull-down assays showed the binding of PPAR $\gamma$  to the C-terminal region comprising kinase domain (291aa–591aa) of PAK4 (Figure 3E), and indicate that the N-terminal CRIB domain is not essential for PAK4/PPAR $\gamma$  binding (Figure 3F).

Next, to determine the functional implication of PAK4-PPAR $\gamma$  binding, we examined if PAK4 was recruited to the PPRE consensus sites and regulates PPAR $\gamma$ -mediated transcriptional activity. Incubation of the binding reaction with either PAK4 or PPAR $\gamma$  antibodies in EMSA assays resulted in supershift of the oligonucleotide mobility further confirming that PAK4 is recruited to the PPAR $\gamma$  consensus binding sequences (Figure 3G).

### **IR-treatment elevates PAK4/PPAR $\gamma$ complex recruitment to PPRE site on Nox1 promoter**

Having confirmed PAK4/PPAR $\gamma$  binding, we next investigated the specific role of PAK4 in regulating PPAR $\gamma$  transcriptional activity and downstream effects on PPAR $\gamma$ -mediated signaling in IR treatments. IP in control and IR-treated cells showed a significant upregulation and complex formation between PAK4 and PPAR $\gamma$  after IR-treatment compared to controls (Figure 4A). Immunocytochemical analysis showed that IR not only significantly elevated the PAK4 nuclear translocation but also induced striking co-localization with PPAR $\gamma$  in glioma cells (Figure 4B). In contrast, untreated-control cells showed very low levels of nuclear-PAK4 and no significant co-localization with PPAR $\gamma$ .

To further evaluate the role of IR-induced nuclear translocation of PAK4 in transcription regulation and possible promoter binding in gliomas, we examined the interaction of PAK4 with specific TF consensus sequences using a protein-DNA interaction array. PAK4, immunoprecipitated from nuclear extracts of control and IR-treated 4910 cells, was incubated with TF-consensus oligonucleotide probe mixtures to determine their interaction with PAK4 on the protein-DNA array. We noted that there was minimal association of nuclear-PAK4 with TF consensus sequence probes in untreated-control cells. In contrast, IR-treated cells showed significant PAK4 binding with different TF consensus elements including an intense binding with those of PPAR $\gamma$  (Figure 4C). These results suggest a notable radiation-induced association of nuclear-PAK4 with PPAR $\gamma$  consensus elements.

PPAR $\gamma$  has been implicated in tumor progression and previous reports showed the modulation of cellular ROS levels by PPAR $\gamma$  agonists.<sup>19, 32</sup> Based on our finding of significant increase in ROS and mesenchymal transition in IR-treated cells, we next investigated a role for PAK4 in modulating PPAR $\gamma$  target genes which regulated ROS in these cells. Nox1 is a key ROS generating NADPH oxidase in cells. When overexpressed in fibroblasts, Nox1 constitutively produces both superoxide and H<sub>2</sub>O<sub>2</sub>, and implicated in malignant transformation, angiogenesis and tumor growth in nude mice.<sup>2, 24</sup> However, regulation of Nox1 expression and its role in gliomas is poorly understood. Immunohistochemical analysis using tissue array revealed a grade dependent increase in Nox1 expression in gliomas with a moderate expression in Grade II and a higher expression

in Grade III and IV GBM tumors (Supplementary Figure S4A, S4B). Radiation significantly elevated Nox1 mRNA levels in both 4910 and 5310 cells (Figure 5A). Immunoblot and confocal studies showed high Nox1 levels in IR-treated cells when compared to controls (Figure 5B & Supplementary Figure S4C). Conversely, PAK4 silencing inhibited Nox1 levels in both cell lines (Figure 5C). Promoter analysis indicated the presence of seven potential PPRE sites in the promoter, exon-1 and intron-1 regions of Nox1 (Figure 5D, Supplementary Table S1). ChIP assays revealed an increased PPAR $\gamma$  binding at R-2 region of the Nox1 promoter 24-hour after IR-treatment in glioma cells (Figure 5E). Moreover, ChIP and re-ChIP assays confirmed PAK4 recruitment to the Nox1 promoter along with PPAR $\gamma$ , which is further elevated in IR-treated cells (Figure 5F). These studies confirm the association of nuclear-PAK4 with PPAR $\gamma$  and suggest a direct recruitment of PAK4/PPAR $\gamma$  complex on Nox1 promoter, which further leads to the increased transcription of Nox1 after radiation in glioma cells.

### **PAK4 is essential for PPAR $\gamma$ -mediated induction of Nox1 and ROS and for IR-induced EMT in glioma cells**

To confirm the role of PAK4 in IR-induced EMT, we further treated SV- and PAK4sh-transfected glioma cells with IR for an additional 24 hours, and analyzed EMT marker expression. Upon IR-treatment, SV-transfected cells showed the expected increase in levels of PPAR $\gamma$ , Nox1 and N-cadherin (Figure 6A). In contrast, PAK4sh-treated cells showed significant attenuation of IR-induced elevation in N-cadherin expression. In addition, PAK4-knockdown also reversed the elevation of Nox1 and N-cadherin expression in PPAR $\gamma$ -FL cells indicating that PAK4 is essential for PPAR $\gamma$ -mediated Nox1 and EMT in glioma cells (Figure 6B). To investigate if PAK4 nuclear localization is essential for Nox1-mediated mesenchymal transition, we overexpressed the NLS mutant of PAK4 (PAK4-NLS-Mut) in 4910 and 5310 cells. There was an obvious increase in cellular Nox1 and N-cadherin expression levels and decreased E-cadherin in PAK4-FL-treated cells, when compared to control- and EV-treatments. On the other hand, overexpression of PAK4-NLS-Mut failed to modulate the expression levels of these proteins (Supplementary Figure S5A). IP experiments revealed that there was no change in the nuclear expression of PAK4 and its binding with PPAR $\gamma$  in PAK4-NLS-Mut-treated 4910 cells, and thus indicate that nuclear translocation of PAK4 is essential for interaction with PPAR $\gamma$  and to regulate Nox1-mediated mesenchymal transition in glioma (Supplementary Figure S5B). Independent treatments with PAK inhibitor II PF-3758309 decreased PAK4 and p-PAK4 levels and significantly inhibited N-cadherin and Slug expression levels which indicate that pharmacological inhibition of PAK4 also suppressed mesenchymal phenotype in glioma cell lines (Supplementary Figure S5C). Further, to confirm the critical roles of PAK4 and PPAR $\gamma$  in the regulation of IR-induced ROS generation in glioma cells, we performed combination treatments of IR with SV, PAK4sh or GW9662 (PPAR $\gamma$  inhibitor). IR-induced ROS levels were significantly suppressed by independent treatments of GW9662 or PAK4sh in 4910 cells (Figure 6C) suggesting that IR-induced ROS elevation and EMT is mediated by the PAK4/PPAR $\gamma$  axis in glioma.

To further confirm the regulation of ROS and EMT by PAK4, we subjected glioma cells to either oxidative stress using H<sub>2</sub>O<sub>2</sub> or to anti-oxidants using NAC in independent experiments

and assessed N-cadherin expression. ROS induction and N-cadherin expression in response to H<sub>2</sub>O<sub>2</sub> treatment was significantly lower in PAK4sh-treated cells compared with SV-treated controls (Supplementary Figure S6A, S6B). Conversely, NAC treatment reduced basal ROS levels and inhibited N-cadherin expression in SV-treated cells, whereas PAK4 overexpression rescued these levels in PAK4-FL-treated glioma cells (Supplementary Figure S6C, S6D). These results confirm the role of nuclear-PAK4 as a key regulator of IR-induced EMT and demonstrate that its interaction with PPAR $\gamma$  and subsequent regulation of ROS through Nox1 expression is critical for activating EMT in gliomas.

### PAK4 downregulation inhibits orthotopic tumor growth in nude mice

In order to validate the *in vitro* findings, we determined the effect of PAK4 downregulation *in vivo* by implantation of stable SV- or PAKsh-transfected 4910 glioma cells in an orthotopic xenograft mouse model. SV-control cells formed prominent intracranial tumors in mice whereas PAK4sh-derived tumors were significantly smaller in size (~49%, Figure 7A). In addition, a combination of IR-treatment on PAK4sh-tumors further decreased the tumor size to (~41%). Immunohistochemical and confocal analyses of PAK4sh-tumor sections showed lower levels of PAK4, PPAR $\gamma$  and Nox1 levels compared with SV-control tumors (Figure 7B). Radiation therapy enhanced the *in vivo* expression of PAK4, PPAR $\gamma$  and Nox1 along with N-cadherin in control tumors suggesting induction of EMT (Figure 7C). In contrast, IR-induced N-cadherin expression was significantly decreased in PAK4sh tumors. These results strongly support a role of PAK4 in controlling tumor growth *in vivo* by PPAR $\gamma$ -mediated EMT after IR and indicate the potential therapeutic approach of targeting PAK4 in combination with radiation treatment in tumors.

## Discussion

Growing evidence suggests that malignant cells adopt EMT as a mechanism to develop resistance to a variety of treatments; hence in epithelial tumors such as glioblastoma, mechanisms of mesenchymal transition have emerged as drivers of resistance and as relevant targets for therapeutic intervention against such malignancies.<sup>23, 29, 40</sup> In particular, radiation therapy in the treatment of malignancies results in the selection of a subpopulation of cells with stem-like and mesenchymal characteristics that survive this treatment and can contribute to tumor progression and adaptive resistance<sup>6, 14</sup>. The molecular mechanisms of these adaptations are poorly understood and are potentially key targets for overcoming tumor resistance. We have previously shown that PAK4 is expressed in high levels in gliomas in a grade-dependent manner and has a potential role in the regulation of cell proliferation and anoikis resistance<sup>26</sup>. We also observed decreased migration and invasion in PAK4-knockdown cells suggesting that PAK4 may play a significant role in processes such as EMT. Based on these results, we hypothesized that PAK4 would have a key role in expression of mesenchymal characteristics in gliomas. We also assessed if PAK4 contributes to radiation-induced EMT and determined the mechanisms that mediate the regulation of EMT by PAK4 in this setting. We observed that PAK4 downregulation leads to loss of mesenchymal phenotype in these cells suggesting a key role for PAK4 in the regulation of EMT. A key finding of this study was the nuclear localization of PAK4 after exposure to IR which appeared to be essential for the transcriptional function of the protein. Our results

show for the first time that the nuclear translocation of PAK4 after IR leads to increased binding to PPAR $\gamma$  as a first step in its regulation of EMT. Although, PAK4 function was shown to be associated with its kinase activity,<sup>8, 57, 63</sup> our present experiments with a kinase-dead PAK4 mutant indicated that the PAK4 physical interaction with PPAR $\gamma$  and the subsequent regulation of mesenchymal transition in glioma cells is independent of its kinase activity. Our results were in corroboration with earlier report which demonstrated that PAK4 could promote transformation, cell migration and tumorigenesis by a kinase-independent mechanism.<sup>38</sup> PAK4 direct interaction with Gab1 was shown to be independent of its kinase-activity. Previous studies have shown that PAK4 could interact with RhoU and regulate cell adhesion and migration in a kinase-independent mechanism in breast cancer cells.<sup>12, 46</sup> In addition, abrogation of PAK4 nuclear localization using PAK4-NLS-Mut plasmid failed to elevate the expression levels of Nox1 and N-cadherin in these cells. Together, our results unequivocally demonstrate that the nuclear PAK4/PPAR $\gamma$  complex binds to the PPAR consensus elements on the *Nox1* promoter after IR resulting in transcriptional upregulation of Nox1 and increase in ROS levels; these findings are associated with induction of EMT and provide a novel mechanism mediated by PAK4 in IR-mediated EMT.

PPAR $\gamma$  has been shown to induce EMT physiologically through a MEK/ERK1/2 pathway in normal intestinal epithelial cells which express high levels of this protein<sup>11</sup>. High expression of PPAR $\gamma$  has also been well-documented in several cancers including glioma<sup>10, 43</sup>. Functional relevance of PPAR $\gamma$  expression in malignancies is recognized to be complex with the observation that it has both oncogenic and tumor suppressor roles depending on cellular context<sup>43</sup>. Downregulation of PPAR $\gamma$  or treatment with antagonist GW9662 suppressed growth in cancer cells suggesting a tumor-promoting role for PPAR $\gamma$  in these cells.<sup>31, 41, 53, 66</sup> PPAR $\gamma$  was shown to protect ErbB2-positive breast cancer cells from palmate-induced toxicity and played a key role in the maintenance of stemness in these cells.<sup>62</sup> Conversely, PPAR $\gamma$  agonists were shown to inhibit tumor growth and cause apoptosis in breast cancer cells although it is unclear if these agonists had a PPAR $\gamma$ -independent effect.<sup>27, 52</sup> We demonstrate that IR induces PPAR $\gamma$  upregulation which associates with nuclear-PAK4 and triggers EMT. These results provide a new context for PPAR $\gamma$ -mediated Nox1 activation in the setting of radiation-induced EMT and demonstrate a PAK4 facilitated tumor promoting function for PPAR $\gamma$  in gliomas. Accumulating evidences indicate the occurrence of mesenchymal transition in glioblastoma and the transcription factors Stat3, C/EBP $\beta$  and transcriptional coactivator TAZ were identified as master regulators mesenchymal gene network activation in these tumors.<sup>5, 9</sup> Individual or combined silencing of Stat3 and C/EBP $\beta$  TFs severely inhibited the mesenchymal gene expression, and decreased the invasive abilities and mesenchymal transition in glioma cells.<sup>9</sup> Our parallel investigation also showed a significant decrease in Stat3 phosphorylation and C/EBP $\beta$  levels upon in PAK4-knockdown in glioma cells, which suggest a potential cross-talk of PAK4 with Stat3 or C/EBP $\beta$  signaling pathways in connection with regulation of mesenchymal gene signature in gliomas. These results are similar to a recent report which showed a significant suppression of Stat3 transcriptional activity and inhibition of stem-like properties in pancreatic cancer cell lines.<sup>60</sup> On the other hand, PPAR $\gamma$  is known to interact with C/EBP factors  $\alpha$  and  $\beta$ , and cooperatively regulate the gene expression in mouse



adipocytes.<sup>33</sup> Hence, the downregulation of C/EBP $\beta$  in PAK4-silenced glioma cells is intriguing although its functional relevance in glioma remains to be better defined.

Basal ROS levels are essential for the regulation of redox-dependent intracellular signaling mechanisms in normal cells whereas increased ROS can lead to oxidative damage and death,<sup>54</sup> in contrast, tumor cells can display persistent elevation of ROS which is implicated as a critical mediator of tumor progression and has been associated with the oncogene-mediated cell transformation, disease progression and poor prognosis in cancer.<sup>47, 59</sup> Elevated ROS facilitates tumor cells to escape detachment-induced death during invasion and metastases and known to play a critical role in EMT.<sup>45, 64</sup> Nox1 is a key regulator of ROS and has been shown to increase ROS levels and activate oxidative stress signaling to modulate anchorage-independent growth, cellular transformation and tumor formation. Recent studies also indicated the critical role of Nox1 in neoplastic transformation of epithelial cells, and regulation of EMT and invasion in melanoma cells.<sup>37</sup> However, a role for Nox1 in regulation of ROS in glioma or its contribution to radiation-induced cellular changes has not been reported. Our results show a novel transcriptional regulation of Nox1 and ROS by PAK4 binding with PPAR $\gamma$ -DNA complex, which is, significantly enhanced in IR-treated cells (Figure 7D). The results of increased ROS generation in glioma cells was countered by antioxidants, a result which is similar to previous reports that ROS expression in cancer cells can be counterbalanced by abundant expression and activation of antioxidant enzymes in order to maintain redox balance.<sup>54</sup>

Of note, large scale genome-wide expression profiling of GBM have delineated subtypes such as classical, neural, proneural and mesenchymal which had potential correlation with clinical outcome.<sup>7, 17, 49, 61</sup> The mesenchymal subtype of GBM has been associated with worse clinical outcome and with more aggressive behavior including increased angiogenesis and invasiveness as well as chemo and radio-resistance.<sup>17, 49, 61</sup> The relationship between the mesenchymal GBM subtype defined by expression profiling and the EMT phenotype defined by biological behavior and protein expression seen in recurrent and treatment resistant GBMs is unclear. However, recent studies have shown that the mesenchymal GBM subtype had the highest correlation with the EMT signature compared with the other GBM subtypes.<sup>65</sup> A mesenchymal transition has also been described in GBM<sup>5</sup> which appears to be driven by a transcriptional mechanism through specific master transcription factors.<sup>9</sup> A similar correlation was reported in a study of glioma stem cells and their association with a mesenchymal transcriptomal signature which correlated with a more aggressive phenotype;<sup>5</sup> the mesenchymal transformation of proneural GBMs is associated with radioresistance similar to the results seen in our study.

In summary, our studies demonstrate a hitherto unreported binding of nuclear-PAK4 with PPAR $\gamma$  and characterize a novel regulation of PPAR $\gamma$ -mediated EMT by PAK4 after IR-treatment both *in vitro* and *in vivo*. These findings provide a mechanistic understanding of IR mediated EMT and the critical role of nuclear-PAK4 in such adaptive resistance mechanisms activated by gliomas in response to radiation therapy. They also provide a strong rationale for therapeutic targeting of PAK4 and PPAR $\gamma$  in the treatment of glioma.

## Materials and methods

### Cell lines, reagents and plasmids

The highly invasive human glioma xenograft cell lines 4910 and 5310 (kindly provided by Dr. David James, University of California, San Francisco)<sup>18</sup> were passaged *in vivo* in mouse brain and cultured in RPMI supplemented with 10% fetal bovine serum (Invitrogen Corporation, Carlsbad, CA), 50 units/ml penicillin and 50 µg/ml streptomycin (Life Technologies, Inc., Frederick, MD). The human GBM cell lines SNB19, U251 and U87 MG were purchased from American Type Culture Collection (ATCC, Rockville, MD) and maintained in DMEM-F12 medium and cells were cultured by incubation in a humidified 5% CO<sub>2</sub> chamber at 37 °C. Antibodies were obtained commercially for the indicated targets as indicated: PAK4, phospho-PAK4 (Ser474), Nox1, E-cadherin, Zo-1, N-cadherin, vimentin, Slug, Stat3, phospho-STAT3(Tyr705, Ser727), C/EBPβ, GAPDH, HDAC-1, anti-FLAG (DYKDDDK tag) (Cell Signal Technology, Beverly, MA), PPARγ (Abcam, Cambridge, MA), normal rabbit IgG, horseradish peroxidase conjugated secondary antibodies (Santa Cruz Biotechnology), and Alexa Fluor® conjugated secondary antibodies (Life Technologies). We also purchased hydrogen peroxide (H<sub>2</sub>O<sub>2</sub>), N-acetyl cysteine (NAC), 2',7'-Dichlorofluorescein Diacetate (H<sub>2</sub>DCFDA), GW9662 (a selective PPARγ inhibitor, Sigma-Aldrich, Carlsbad, CA) and PAK inhibitor II PF-3758309 (Millipore, Billerica, MA), and used in the present study. The human PAK4.shRNA plasmid (PAK4sh) comprising a pool of three different targeting shRNAs (sc-39060-SH) and specific scrambled shRNA vector (SV) (Santa Cruz Biotechnology, Santa Cruz, CA), full-length GFP-tagged PAK4 overexpression plasmid (PAK4-FL) (Origene, Rockville, MD), kinase-dead PAK4 plasmid (PAK4-K350M),<sup>1</sup> PAK4 NLS mutant plasmid (NLS1, Lysine mutated to Alanine within 4–8 aa) (PAK4-NLS-Mut), GST-tagged PPARγ (GST-PPARγ; Addgene plasmid 16549)<sup>21</sup>, FLAG-tagged PPARγ (FLAG-PPARγ; Addgene plasmid 8895)<sup>20</sup> and respective empty vector controls were used in the study.

### Transfection, inhibitor and radiation treatments

Cells were seeded ( $0.5 \times 10^6$ ) in 100 mm plates and serum-starved for 6 hours before transfection with shRNA or overexpression plasmids or respective control (SV or EV) vectors using X-tremeGENE 9 DNA Transfection Reagent (Roche, Nutley, NJ). Cells were collected after 48 hours of transient transfection for all *in vitro* experiments. For *in vivo* experiments, stable expressing 4910 clones of SV and PAK4sh plasmids were selected and maintained in puromycin (500µg/L) medium. The RS2000 Biological Irradiator (Rad Source Technologies, Inc., Boca Raton, FL) x-ray unit operated at 150 kV/50 mA and delivering 0.71 Gy/min was used for radiation treatments.<sup>3</sup> Cells were irradiated with a single dose of 8 Gy, and for combination experiments, cells were treated with plasmids or inhibitors for 24 hours followed by IR treatment for another 24 hours, at the end of which cells were collected for further analysis.

### Real-time PCR, ChIP and re-ChIP assays

Total RNA was isolated from cells using TRIZOL reagent and cDNAs were synthesized from 1µg of RNA samples using the SuperScript® III Reverse Transcriptase cDNA synthesis kit (Life Technologies, Carlsbad, CA). Real-time quantitative PCR was performed

as described earlier<sup>26</sup> with the following parameters: 1 cycle of 95 °C-10 min, 40 cycles of 95 °C for 15 s, 60 °C for 30 s, 72 °C for 30 s and 1 cycle of 72 °C for 10 min. Data were analyzed using iCycler IQ version-3.1 software (Bio-Rad Laboratories, Hercules, CA) and Ct values were converted into fold change of expression using  $2^{-\Delta\Delta Ct}$  method ( $\Delta\Delta Ct = \Delta Ct$  of treatment -  $\Delta Ct$  of control). Standard ChIP assays were performed with anti-PPAR $\gamma$ , anti-PAK4 or normal rabbit IgG antibodies using a commercially available ChIP-IT Express Magnetic Chromatin-Immunoprecipitation kit (Active Motif, Carlsbad, CA) following to manufacturer's protocol, and ChIPed DNA was used for normal or quantitative PCR. For re-ChIP analyses, the immunoprecipitated chromatin from the first antibody is eluted from the protein magnetic beads. Eluted chromatin from primary ChIP reaction was dissociated with high salt buffer and then desalted with a column supplied with Active motif Re-ChIP-IT® kit. After desalting, recovered DNA was diluted 10-fold with the Re-ChIP buffer and used for a second round of ChIP with second antibody. Re-ChIP DNA was amplified with real-time PCR with gene-specific primers (n=5). The following gene-specific ChIP PCR primers were used to amplify Nox1 promoter region (R-1) sense 5'-TACATGAAAATGAAAAAGGCCAAGA-3' (112 bp), antisense 5'-TGTTCTTCAAGAGTGCTTTGG-3'; R-2, sense 5'-CCAAAGCACTCTTGAAGACA-3', antisense 5'-CGGAGCTCTCCATTCAGTTC-3' (101 bp); exon-1 region (R-3) sense 5'-GGACAAATGTTCCATTCCTGA-3', antisense 5'-CCCAGTTTCCCATTGTCAAG-3' (105 bp); intron-1 region (R-4) sense 5'-CCACTGGTTTTTCAGTTTTGTTTC-3', antisense 5'-CTGGTCTTGATGAGCCCAAT-3' (146 bp). Pre-immunoprecipitated DNA (5% of sample) was used as an input control in each reaction. Specific GAPDH primers, sense 5'-CGGTGCGTGCCCAGTTG-3' and antisense-5'-GCGACGCAAAGAAGATG-3' were used for input PCR. The relative-ChIP amplification levels of each fragment were presented as a percentage of total inputs in a total of five repetitions and three independent experiments and the statistical significance was denoted at  $p \leq 0.05$  or  $p \leq 0.01$ .

### Western blotting, immunoprecipitation and EMSA

Nuclear and cytoplasmic fractions were separated using Nuclear Extract Kit following manufacturer's instructions (Active Motif, Carlsbad, CA), and whole cell lysates were isolated using RIPA buffer supplemented with protease and phosphatase inhibitor cocktails (Sigma-Aldrich, Carlsbad, CA) as described earlier<sup>26</sup>. Immunoprecipitation was performed with nuclear extracts (500  $\mu$ g) by incubating with specific antibodies against PAK4, PPAR $\gamma$  and non-specific IgG using  $\mu$ MACS protein-G microbeads and MACS Separation Columns following the manufacturer's instructions (Miltenyi Biotec, Auburn, CA). Electrophoretic mobility shift assays were performed with 5 $\mu$ g of nuclear extract to detect PPAR $\gamma$  DNA binding using EMSA Kit (Panomics) following manufacturer's instructions. For supershift assay, specific antibodies against PAK4, PPAR $\gamma$  and IgG (2  $\mu$ g) were pre-incubated with nuclear protein for 30 min before the addition of biotin-labeled probe. TF-TF interaction arrays and protein-DNA interaction arrays were performed using immunoprecipitated PAK4 from nuclear lysates of 4910 cells (Panomics, Fremont, CA) and described in detail in Supplementary Information.

### ***In vitro* transcription & translation and GST pull-down experiments**

The PAK4 truncated mutants were synthesized *in vitro* with specific PCR-amplified fragments using Transcend Biotin-Lysyl-tRNA and TnT Quick Coupled Transcription/Translation System (Promega, Madison, WI) following the manufacturer's instructions. The recombinant GST and GST-tagged PPAR $\gamma$  fusion protein was expressed bacterially following induction with IPTG (1.0 mg/ml) and was purified using MagneGST Pull-Down System (Promega) following manufacturer's protocol and verified by SDS-PAGE. About ~2  $\mu$ g aliquots of protein-coated GST particles were incubated with biotin-labeled PAK4 truncated mutants overnight at 4°C. Beads were washed for 2–3 times, eluted in 20  $\mu$ l of pre-heated sample buffer, separated on SDS-PAGE, transferred to nitrocellulose membrane. The *in vitro* protein binding was detected with Transcend Nonradioactive Translation Detection Systems following manufacturer's instructions.<sup>26</sup>

### **Total ROS estimation**

Total cellular ROS levels were measured using the fluorescent cell-permanent probe, 2',7'-dichlorodihydrofluorescein diacetate (H<sub>2</sub>DCFDA) (Sigma-Aldrich) as described previously<sup>13</sup>. Approximately  $0.5 \times 10^4$  cells were plated in 96-well plates and subjected to transfection and IR treatments as described above. In the combination treatments, cells were also treated with 10  $\mu$ M H<sub>2</sub>O<sub>2</sub> or 0.1 mM N-acetyl cysteine (NAC) or 10  $\mu$ M GW9662 for additional 24 hours. At the end of the treatments, H<sub>2</sub>DCFDA (10  $\mu$ M/L) was added to the medium, the cells incubated for 30 min at 37°C and fluorescent signal was examined by confocal microscopy and measured using microplate reader.

### ***In vivo* tumor experiments**

Orthotopic tumor experiments were performed in 6–8 week old athymic female nude mice following the Institutional Animal Care and Use Committee (IACUC) approved protocols of all surgical interventions and post-operative animal care. The 4910 cells with stable expression of SV and PAK4sh plasmids ( $1 \times 10^6$  cells/10  $\mu$ l of 1 $\times$ PBS) were intracranially implanted (depth of 3–4 mm) in nude mice. Tumors were allowed to grow for 10 days and each group was further separated in to 2 treatment groups (n=6) and one group was subjected to three IR doses (8 Gy) on alternate days as described earlier.<sup>26</sup> After IR-treatment, mice were monitored and euthanized when symptoms of tumor burden including trouble in feeding or grooming or loss of >20% of body weight were evident. The experiment was terminated after 60 days; mice brains were resected, fixed in 10% formalin and embedded in paraffin blocks. Every fifth section (5  $\mu$ m) in series was H&E stained and the tumor volumes were calculated with Image Pro Discovery Program software (Media Cybernetics, Inc., Silver Spring, MD) as detailed previously<sup>3</sup>.

### **Statistical analysis**

The data obtained from three independent experiments was analyzed with unpaired two-sided Student's t test (Sigmastat 3.1, SPSS Inc. Chicago, IL), represented as mean  $\pm$  SD and significance was indicated by  $p \leq 0.05$  and  $p \leq 0.01$ . Densitometric analysis was performed using ImageJ 1.42 (NIH) software.

## Supplementary Material

Refer to Web version on PubMed Central for supplementary material.

## Acknowledgments

We thank Jihong Xu, Krishna K. Veeravalli and Bharath Chelluboina for technical help. We greatly appreciate Dr. Annie N. Y. Cheung (University of Hong Kong, Hong Kong) and Dr. Audrey Minden (Rutgers University, NJ) for kindly providing the PAK4-NLS-Mut and PAK4-K350M plasmids respectively, for our studies. We thank Drs. Deepa Sampath and Rosa Lapalombella for manuscript review and helpful comments. This project was supported by the Ohio State University Pelotonia Fellowship (DK), NCI grant 5K24CA160777 (VKP), the Sanford/Rife Family Glioblastoma Research Fund and the Snyder Nation Foundation.

## References

1. Abo A, Qu J, Cammarano MS, Dan C, Fritsch A, Baud V, et al. PAK4, a novel effector for Cdc42Hs, is implicated in the reorganization of the actin cytoskeleton and in the formation of filopodia. *EMBO J.* 1998; 17:6527–6540. [PubMed: 9822598]
2. Arbiser JL, Petros J, Klapfer R, Govindajaran B, McLaughlin ER, Brown LF, et al. Reactive oxygen generated by Nox1 triggers the angiogenic switch. *Proc Natl Acad Sci U S A.* 2002; 99:715–720. [PubMed: 11805326]
3. Badiga AV, Chetty C, Kesanakurti D, Are D, Gujrati M, Klopfenstein JD, et al. MMP-2 siRNA inhibits radiation-enhanced invasiveness in glioma cells. *PLoS One.* 2011; 6:e20614. [PubMed: 21698233]
4. Baldassa S, Calogero AM, Colombo G, Zippel R, Gnesutta N. N-terminal interaction domain implicates PAK4 in translational regulation and reveals novel cellular localization signals. *J Cell Physiol.* 2010; 224:722–733. [PubMed: 20578242]
5. Bhat KP, Salazar KL, Balasubramanian V, Wani K, Heathcock L, Hollingsworth F, et al. The transcriptional coactivator TAZ regulates mesenchymal differentiation in malignant glioma. *Genes Dev.* 2011; 25:2594–2609. [PubMed: 22190458]
6. Brabletz T. To differentiate or not--routes towards metastasis. *Nature reviews Cancer.* 2012; 12:425–436. [PubMed: 22576165]
7. Brennan CW, Verhaak RG, McKenna A, Campos B, Nounshmehr H, Salama SR, et al. The somatic genomic landscape of glioblastoma. *Cell.* 2013; 155:462–477. [PubMed: 24120142]
8. Callow MG, Zozulya S, Gishizky ML, Jallal B, Smeal T. PAK4 mediates morphological changes through the regulation of GEF-H1. *J Cell Sci.* 2005; 118:1861–1872. [PubMed: 15827085]
9. Carro MS, Lim WK, Alvarez MJ, Bollo RJ, Zhao X, Snyder EY, et al. The transcriptional network for mesenchymal transformation of brain tumours. *Nature.* 2010; 463:318–325. [PubMed: 20032975]
10. Chattopadhyay N, Singh DP, Heese O, Godbole MM, Sinohara T, Black PM, et al. Expression of peroxisome proliferator-activated receptors (PPARS) in human astrocytic cells: PPARgamma agonists as inducers of apoptosis. *J Neurosci Res.* 2000; 61:67–74. [PubMed: 10861801]
11. Chen L, Necela BM, Su W, Yanagisawa M, Anastasiadis PZ, Fields AP, et al. Peroxisome proliferator-activated receptor gamma promotes epithelial to mesenchymal transformation by Rho GTPase-dependent activation of ERK1/2. *J Biol Chem.* 2006; 281:24575–24587. [PubMed: 16815847]
12. Dart AE, Box GM, Court W, Gale ME, Brown JP, Pinder SE, et al. PAK4 promotes kinase-independent stabilization of RhoU to modulate cell adhesion. *J Cell Biol.* 2015; 211:863–879. [PubMed: 26598620]
13. Davison CA, Durbin SM, Thau MR, Zellmer VR, Chapman SE, Diener J, et al. Antioxidant enzymes mediate survival of breast cancer cells deprived of extracellular matrix. *Cancer Res.* 2013; 73:3704–3715. [PubMed: 23771908]
14. De Craene B, Bercx G. Regulatory networks defining EMT during cancer initiation and progression. *Nature reviews Cancer.* 2013; 13:97–110. [PubMed: 23344542]

15. Dummler B, Ohshiro K, Kumar R, Field J. Pak protein kinases and their role in cancer. *Cancer Metastasis Rev.* 2009; 28:51–63. [PubMed: 19165420]
16. Evans RM, Barish GD, Wang YX. PPARs and the complex journey to obesity. *Nat Med.* 2004; 10:355–361. [PubMed: 15057233]
17. Frattini V, Trifonov V, Chan JM, Castano A, Lia M, Abate F, et al. The integrated landscape of driver genomic alterations in glioblastoma. *Nat Genet.* 2013; 45:1141–1149. [PubMed: 23917401]
18. Giannini C, Sarkaria JN, Saito A, Uhm JH, Galanis E, Carlson BL, et al. Patient tumor EGFR and PDGFRA gene amplifications retained in an invasive intracranial xenograft model of glioblastoma multiforme. *Neuro Oncol.* 2005; 7:164–176. [PubMed: 15831234]
19. Han EJ, Im CN, Park SH, Moon EY, Hong SH. Combined treatment with peroxisome proliferator-activated receptor (PPAR) gamma ligands and gamma radiation induces apoptosis by PPARgamma-independent up-regulation of reactive oxygen species-induced deoxyribonucleic acid damage signals in non-small cell lung cancer cells. *Int J Radiat Oncol Biol Phys.* 2013; 85:e239–e248. [PubMed: 23332223]
20. Hauser S, Adelmant G, Sarraf P, Wright HM, Mueller E, Spiegelman BM. Degradation of the peroxisome proliferator-activated receptor gamma is linked to ligand-dependent activation. *J Biol Chem.* 2000; 275:18527–18533. [PubMed: 10748014]
21. He TC, Chan TA, Vogelstein B, Kinzler KW. PPARdelta is an APC-regulated target of nonsteroidal anti-inflammatory drugs. *Cell.* 1999; 99:335–345. [PubMed: 10555149]
22. Jin R, Liu W, Menezes S, Yue F, Zheng M, Kovacevic Z, et al. The metastasis suppressor NDRG1 modulates the phosphorylation and nuclear translocation of beta-catenin through mechanisms involving FRAT1 and PAK4. *J Cell Sci.* 2014; 127:3116–3130. [PubMed: 24829151]
23. Kahlert UD, Nikkhah G, Maciaczyk J. Epithelial-to-mesenchymal(-like) transition as a relevant molecular event in malignant gliomas. *Cancer Lett.* 2013; 331:131–138. [PubMed: 23268331]
24. Kamata T. Roles of Nox1 and other Nox isoforms in cancer development. *Cancer Sci.* 2009; 100:1382–1388. [PubMed: 19493276]
25. Kesanakurti D, Chetty C, Rajasekhar Maddirela D, Gujrati M, Rao JS. Functional cooperativity by direct interaction between PAK4 and MMP-2 in the regulation of anoikis resistance, migration and invasion in glioma. *Cell Death Dis.* 2012; 3:e445. [PubMed: 23254288]
26. Kesanakurti D, Chetty C, Rajasekhar Maddirela D, Gujrati M, Rao JS. Essential role of cooperative NF-kappaB and Stat3 recruitment to ICAM-1 intronic consensus elements in the regulation of radiation-induced invasion and migration in glioma. *Oncogene.* 2013; 32:5144–5155. [PubMed: 23178493]
27. Kim KY, Kim SS, Cheon HG. Differential anti-proliferative actions of peroxisome proliferator-activated receptor-gamma agonists in MCF-7 breast cancer cells. *Biochem Pharmacol.* 2006; 72:530–540. [PubMed: 16806087]
28. Komatsu D, Kato M, Nakayama J, Miyagawa S, Kamata T. NADPH oxidase 1 plays a critical mediating role in oncogenic Ras-induced vascular endothelial growth factor expression. *Oncogene.* 2008; 27:4724–4732. [PubMed: 18454179]
29. Kubelt C, Hattermann K, Sebens S, Mehdorn HM, Held-Feindt J. Epithelial-to-mesenchymal transition in paired human primary and recurrent glioblastomas. *Int J Oncol.* 2015; 46:2515–2525. [PubMed: 25845427]
30. Lamouille S, Xu J, Derynck R. Molecular mechanisms of epithelial-mesenchymal transition. *Nat Rev Mol Cell Biol.* 2014; 15:178–196. [PubMed: 24556840]
31. Lee JJ, Drakaki A, Iliopoulos D, Struhl K. MiR-27b targets PPARgamma to inhibit growth, tumor progression and the inflammatory response in neuroblastoma cells. *Oncogene.* 2012; 31:3818–3825. [PubMed: 22120719]
32. Lee KS, Kim SR, Park SJ, Park HS, Min KH, Jin SM, et al. Peroxisome proliferator activated receptor-gamma modulates reactive oxygen species generation and activation of nuclear factor-kappaB and hypoxia-inducible factor 1alpha in allergic airway disease of mice. *J Allergy Clin Immunol.* 2006; 118:120–127. [PubMed: 16815147]
33. Lefterova MI, Zhang Y, Steger DJ, Schupp M, Schug J, Cristancho A, et al. PPARgamma and C/EBP factors orchestrate adipocyte biology via adjacent binding on a genome-wide scale. *Genes Dev.* 2008; 22:2941–2952. [PubMed: 18981473]

34. Lehrke M, Lazar MA. The many faces of PPARgamma. *Cell*. 2005; 123:993–999. [PubMed: 16360030]
35. Li X, Ke Q, Li Y, Liu F, Zhu G, Li F. DGCR6L, a novel PAK4 interaction protein, regulates PAK4-mediated migration of human gastric cancer cell via LIMK1. *Int J Biochem Cell Biol*. 2010; 42:70–79. [PubMed: 19778628]
36. Li Y, Shao Y, Tong Y, Shen T, Zhang J, Li Y, et al. Nucleo-cytoplasmic shuttling of PAK4 modulates beta-catenin intracellular translocation and signaling. *Biochim Biophys Acta*. 2012; 1823:465–475. [PubMed: 22173096]
37. Liu F, Gomez Garcia AM, Meyskens FL Jr. NADPH oxidase 1 overexpression enhances invasion via matrix metalloproteinase-2 and epithelial-mesenchymal transition in melanoma cells. *J Invest Dermatol*. 2012; 132:2033–2041. [PubMed: 22513785]
38. Liu Y, Xiao H, Tian Y, Nekrasova T, Hao X, Lee HJ, et al. The pak4 protein kinase plays a key role in cell survival and tumorigenesis in athymic mice. *Mol Cancer Res*. 2008; 6:1215–1224. [PubMed: 18644984]
39. Lu KV, Chang JP, Parachoniak CA, Pandika MM, Aghi MK, Meyronet D, et al. VEGF inhibits tumor cell invasion and mesenchymal transition through a MET/VEGFR2 complex. *Cancer Cell*. 2012; 22:21–35. [PubMed: 22789536]
40. Mahabir R, Tanino M, Elmansuri A, Wang L, Kimura T, Itoh T, et al. Sustained elevation of Snail promotes glial-mesenchymal transition after irradiation in malignant glioma. *Neuro Oncol*. 2014; 16:671–685. [PubMed: 24357458]
41. Masuda T, Wada K, Nakajima A, Okura M, Kudo C, Kadowaki T, et al. Critical role of peroxisome proliferator-activated receptor gamma on anoikis and invasion of squamous cell carcinoma. *Clin Cancer Res*. 2005; 11:4012–4021. [PubMed: 15930335]
42. Meng J, Li P, Zhang Q, Yang Z, Fu S. A radiosensitivity gene signature in predicting glioma prognostic via EMT pathway. *Oncotarget*. 2014; 5:4683–4693. [PubMed: 24970813]
43. Michalik L, Desvergne B, Wahli W. Peroxisome-proliferator-activated receptors and cancers: complex stories. *Nature reviews Cancer*. 2004; 4:61–70. [PubMed: 14708026]
44. Minden A. The pak4 protein kinase in breast cancer. *ISRN Oncol*. 2012; 2012:694201. [PubMed: 23326684]
45. Nagano O, Okazaki S, Saya H. Redox regulation in stem-like cancer cells by CD44 variant isoforms. *Oncogene*. 2013; 32:5191–5198. [PubMed: 23334333]
46. Paliouras GN, Naujokas MA, Park M. Pak4, a novel Gab1 binding partner, modulates cell migration and invasion by the Met receptor. *Mol Cell Biol*. 2009; 29:3018–3032. [PubMed: 19289496]
47. Park MT, Kim MJ, Suh Y, Kim RK, Kim H, Lim EJ, et al. Novel signaling axis for ROS generation during K-Ras-induced cellular transformation. *Cell Death Differ*. 2014; 21:1185–1197. [PubMed: 24632950]
48. Pestereva E, Kanakasabai S, Bright JJ. PPARgamma agonists regulate the expression of stemness and differentiation genes in brain tumour stem cells. *Br J Cancer*. 2012; 106:1702–1712. [PubMed: 22531638]
49. Phillips HS, Kharbanda S, Chen R, Forrester WF, Soriano RH, Wu TD, et al. Molecular subclasses of high-grade glioma predict prognosis, delineate a pattern of disease progression, and resemble stages in neurogenesis. *Cancer Cell*. 2006; 9:157–173. [PubMed: 16530701]
50. Qu J, Cammarano MS, Shi Q, Ha KC, de Lanerolle P, Minden A. Activated PAK4 regulates cell adhesion and anchorage-independent growth. *Mol Cell Biol*. 2001; 21:3523–3533. [PubMed: 11313478]
51. Radu M, Semenova G, Kosoff R, Chernoff J. PAK signalling during the development and progression of cancer. *Nature reviews Cancer*. 2014; 14:13–25. [PubMed: 24505617]
52. Sawayama H, Ishimoto T, Watanabe M, Yoshida N, Sugihara H, Kurashige J, et al. Small molecule agonists of PPAR-gamma exert therapeutic effects in esophageal cancer. *Cancer Res*. 2014; 74:575–585. [PubMed: 24272485]
53. Schaefer KL, Wada K, Takahashi H, Matsuhashi N, Ohnishi S, Wolfe MM, et al. Peroxisome proliferator-activated receptor gamma inhibition prevents adhesion to the extracellular matrix and

- induces anoikis in hepatocellular carcinoma cells. *Cancer Res.* 2005; 65:2251–2259. [PubMed: 15781638]
54. Schieber M, Chandel NS. ROS function in redox signaling and oxidative stress. *Curr Biol.* 2014; 24:R453–R462. [PubMed: 24845678]
55. Schwartzbaum JA, Fisher JL, Aldape KD, Wrensch M. Epidemiology and molecular pathology of glioma. *Nat Clin Pract Neurol.* 2006; 2:494–503. quiz 491 p following 516. [PubMed: 16932614]
56. Siebzehnrubl FA, Silver DJ, Tugertimur B, Deleyrolle LP, Siebzehnrubl D, Sarkisian MR, et al. The ZEB1 pathway links glioblastoma initiation, invasion and chemoresistance. *EMBO Mol Med.* 2013; 5:1196–1212. [PubMed: 23818228]
57. Siu MK, Chan HY, Kong DS, Wong ES, Wong OG, Ngan HY, et al. p21-activated kinase 4 regulates ovarian cancer cell proliferation, migration, and invasion and contributes to poor prognosis in patients. *Proc Natl Acad Sci U S A.* 2010; 107:18622–18627. [PubMed: 20926745]
58. Stupp R, Mason WP, van den Bent MJ, Weller M, Fisher B, Taphoorn MJ, et al. Radiotherapy plus concomitant and adjuvant temozolomide for glioblastoma. *N Engl J Med.* 2005; 352:987–996. [PubMed: 15758009]
59. Trachootham D, Alexandre J, Huang P. Targeting cancer cells by ROS-mediated mechanisms: a radical therapeutic approach? *Nat Rev Drug Discov.* 2009; 8:579–591. [PubMed: 19478820]
60. Tyagi N, Marimuthu S, Bhardwaj A, Deshmukh SK, Srivastava SK, Singh AP, et al. p-21 activated kinase 4 (PAK4) maintains stem cell-like phenotypes in pancreatic cancer cells through activation of STAT3 signaling. *Cancer Lett.* 2016; 370:260–267. [PubMed: 26546043]
61. Verhaak RG, Hoadley KA, Purdom E, Wang V, Qi Y, Wilkerson MD, et al. Integrated genomic analysis identifies clinically relevant subtypes of glioblastoma characterized by abnormalities in PDGFRA, IDH1, EGFR, and NF1. *Cancer Cell.* 2010; 17:98–110. [PubMed: 20129251]
62. Wang X, Sun Y, Wong J, Conklin DS. PPARgamma maintains ERBB2-positive breast cancer stem cells. *Oncogene.* 2013; 32:5512–5521. [PubMed: 23770845]
63. Whale AD, Dart A, Holt M, Jones GE, Wells CM. PAK4 kinase activity and somatic mutation promote carcinoma cell motility and influence inhibitor sensitivity. *Oncogene.* 2013; 32:2114–2120. [PubMed: 22689056]
64. Wu CH, Tang SC, Wang PH, Lee H, Ko JL. Nickel-induced epithelial-mesenchymal transition by reactive oxygen species generation and E-cadherin promoter hypermethylation. *J Biol Chem.* 2012; 287:25292–25302. [PubMed: 22648416]
65. Zarkoob H, Taube JH, Singh SK, Mani SA, Kohandel M. Investigating the link between molecular subtypes of glioblastoma, epithelial-mesenchymal transition, and CD133 cell surface protein. *PLoS One.* 2013; 8:e64169. [PubMed: 23734191]
66. Zaytseva YY, Wang X, Southard RC, Wallis NK, Kilgore MW. Down-regulation of PPARgamma1 suppresses cell growth and induces apoptosis in MCF-7 breast cancer cells. *Mol Cancer.* 2008; 7:90. [PubMed: 19061500]
67. Zhang H, Li Z, Viklund EK, Stromblad S. P21-activated kinase 4 interacts with integrin alpha v beta 5 and regulates alpha v beta 5-mediated cell migration. *J Cell Biol.* 2002; 158:1287–1297. [PubMed: 12356872]
68. Zheng H, Shen M, Zha YL, Li W, Wei Y, Blanco MA, et al. PKD1 phosphorylation-dependent degradation of SNAIL by SCF-FBXO11 regulates epithelial-mesenchymal transition and metastasis. *Cancer Cell.* 2014; 26:358–373. [PubMed: 25203322]



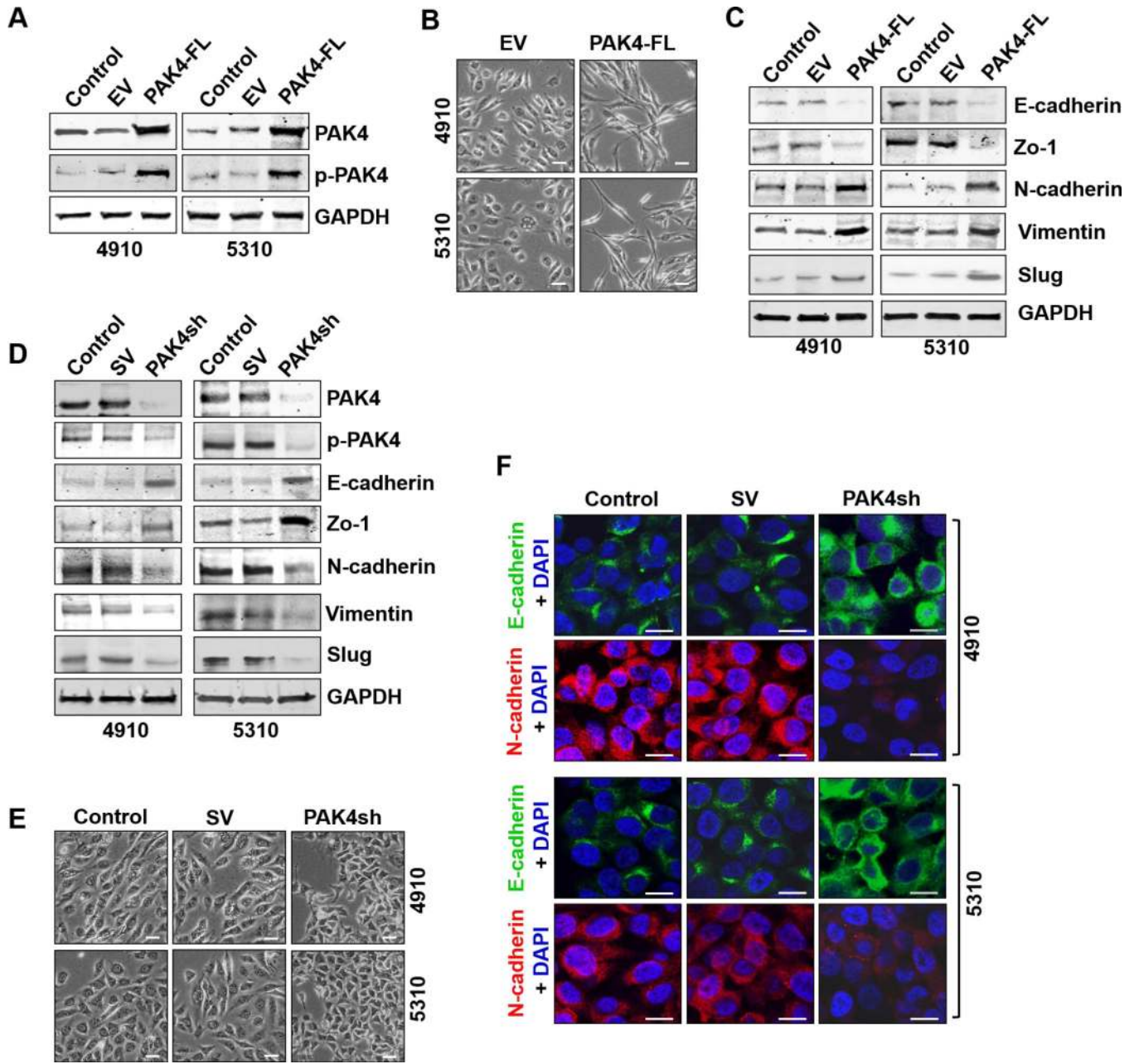


**Figure 1. Effects of PAK4 overexpression and knockdown on mesenchymal transition in glioma cells**

(A) Western blot analysis of 4910 and 5310 glioma cells transfected with EV and PAK4-FL for 48 hours along with untreated controls and GAPDH served as a loading control. (B) Representative micrographs of morphological characteristics in EV- or PAK4-FL-treated glioma cells after 48 hour transfection. Scale bars: 10µm. (C) Representative immunoblots from three independent experiments using whole cell lysates of glioma cells transfected with EV or PAK4-FL to assess changes in EMT markers. (D) Immunoblot analysis of effects of PAK4 downregulation using PAK4shRNA when compared with untreated and SV controls in 4910 and 5310 cells. (E) Phase contrast micrographs of morphological characteristics of

4910 and 5310 cells after SV and PAK4sh treatments for 48 hours. Scale bars: 10 $\mu$ m. **(F)** Confocal microscopy showing E-cadherin (green) and N-cadherin (red) expression in control, SV- and PAK4sh-treated cells. DAPI was used for nuclear counterstaining. Scale bars: 10 $\mu$ m.

Author Manuscript

Author Manuscript

Author Manuscript

Author Manuscript

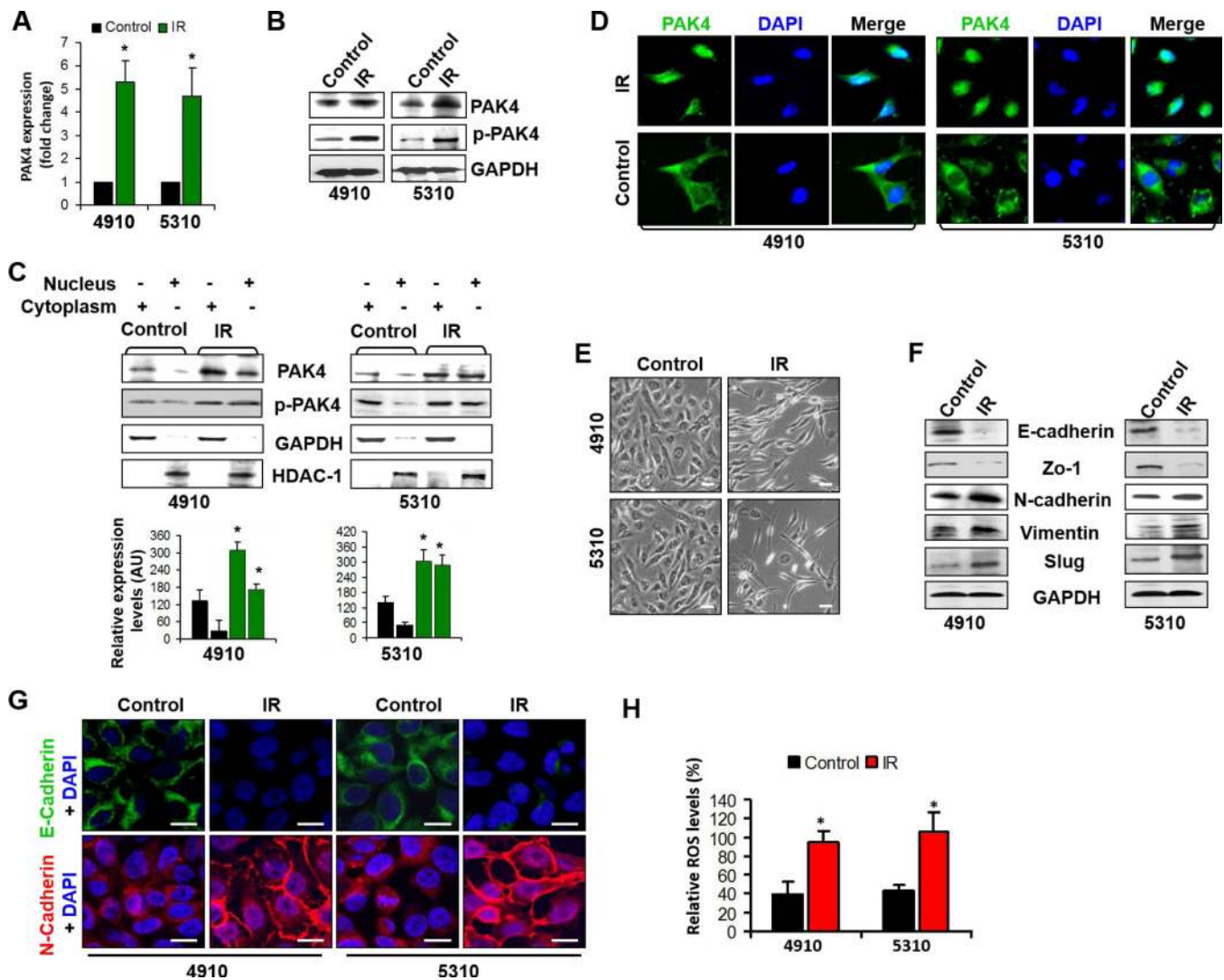


**Figure 2. Radiation-induced nuclear localization of PAK4 and correlation with increased EMT in glioma cells**

(A) PAK mRNA levels in control and IR (8Gy)-treated cells as determined by quantitative PCR. Fold change values of PAK4 are represented as mean  $\pm$  SD of levels obtained from at least five repetitions in three experimental replicates (\* $p$   $\leq$  0.01). (B) Western blotting with cellular lysates showing PAK4 and phospho-PAK4 expression in control and IR (8Gy)-treated cells. (C) Western blot analysis of PAK4 and phospho-PAK4 levels in cytoplasmic and nuclear fractions with or without IR-treatment. GAPDH and HDAC-1 were used as loading controls for cytoplasmic and nuclear fractions respectively. Relative expression levels of cytoplasmic and nuclear-PAK4 were estimated by densitometry (ImageJ 1.42) and mean  $\pm$  SD values were presented (\* $p$   $\leq$  0.01). (D) Immunocytochemical analysis to assess sub-cellular localization of PAK4 in control- and IR (8Gy)-treated cells. Nuclei were counterstained with DAPI. (E) Micrographs showing morphological changes in 4910 and 5310 cells after IR treatments. Scale bars: 10µm. (F) Western blot analysis with whole cell lysates to assess the expression of epithelial and mesenchymal regulator proteins. (G) Confocal microscopy to examine changes in N-cadherin (red) and E-cadherin (green) levels

in IR-treated cells after 48 hours. Nuclei were counterstained with DAPI. Scale bars: 10 $\mu$ m. **(H)** Assessment of total cellular ROS content in control and IR-treated cells with H<sub>2</sub>DCFDA staining as described in Materials and Methods 48-hour after IR treatment. Relative ROS levels from three independent experiments are shown as mean  $\pm$  SD (\*p  $\leq$  0.01).

Author Manuscript

Author Manuscript

Author Manuscript

Author Manuscript

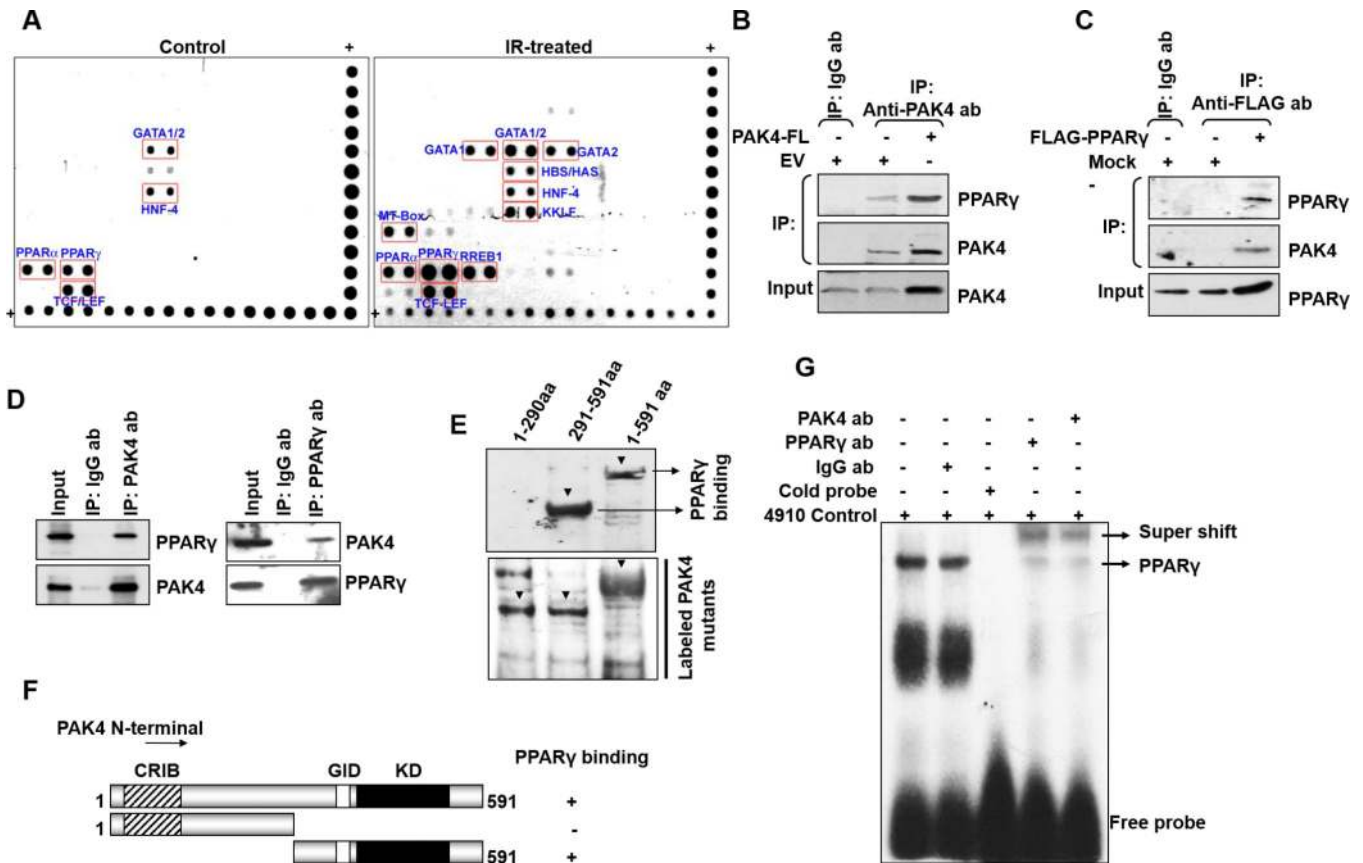


**Figure 3. Association of PAK4 with PPAR $\gamma$  in the nuclear compartment**

(A) Identification of potential PAK4 associating TFs using TF-TF Interaction Array. PAK4 was immunoprecipitated from nuclear extracts of 4910 cells with anti-PAK4 antibody and used as a bait. Isotype-specific IgG precipitates were used as negative control. PAK4 association with various TFs is identified as horizontal duplicate spots on the x-ray film. “+” indicates the positive control signals. (B) 4910 cells were treated with EV and PAK4-FL for 48 hours and IP experiments was performed with nuclear lysates (500  $\mu$ g) from 4910 cells with specific antibodies against PAK4 and non-specific IgG followed by immunoblotting with PPAR $\gamma$ . Inputs indicate 10% of each pre-IP samples. (C) PPAR $\gamma$  IP using anti-FLAG and anti-IgG antibody from nuclear lysates of 4910 cells at 48 hours post-transfection with EV or FLAG-PPAR $\gamma$  constructs followed by immunoblotting for PAK4. (D) IP experiments using 4910 lysates with either a PAK4 specific antibody or non-specific IgG followed by immunoprobng for PPAR $\gamma$ . Reciprocal IPs were performed with anti-PPAR $\gamma$  antibody and subsequent immunoblotting with PAK4 to confirm PAK4/PPAR $\gamma$  association in the nucleus. (E) Identification of minimal PPAR $\gamma$ -interaction domain of PAK4 using bacterially expressed GST, and GST-PPAR $\gamma$  purified using MagneGST Pull-Down System following manufacturer’s protocol. Biotin-labeled PAK4 truncated mutants (1–290aa, 291–591aa 1–591aa) were incubated with GST-PPAR $\gamma$ , separated on 10% SDS-PAGE and detected as described in Materials and Methods (Top panel). Inputs (10% samples) were analyzed by SDS-PAGE (Bottom panel). (F) Schematic representation of mapping PPAR $\gamma$  interacting domain on PAK4 using different truncation mutants. CRIB: Cdc42-and Rac-interactive

binding motif; GID: GEF-H1 Interaction Domain; KD: Kinase Domain. (G) EMSA was performed with 4910 Nuclear extracts (5 $\mu$ g) to detect PPAR $\gamma$  activity. For the supershift analyses, specific antibodies against PAK4 and PPAR $\gamma$  were incubated with control sample before adding the biotin-labeled probe.

Author Manuscript

Author Manuscript

Author Manuscript

Author Manuscript

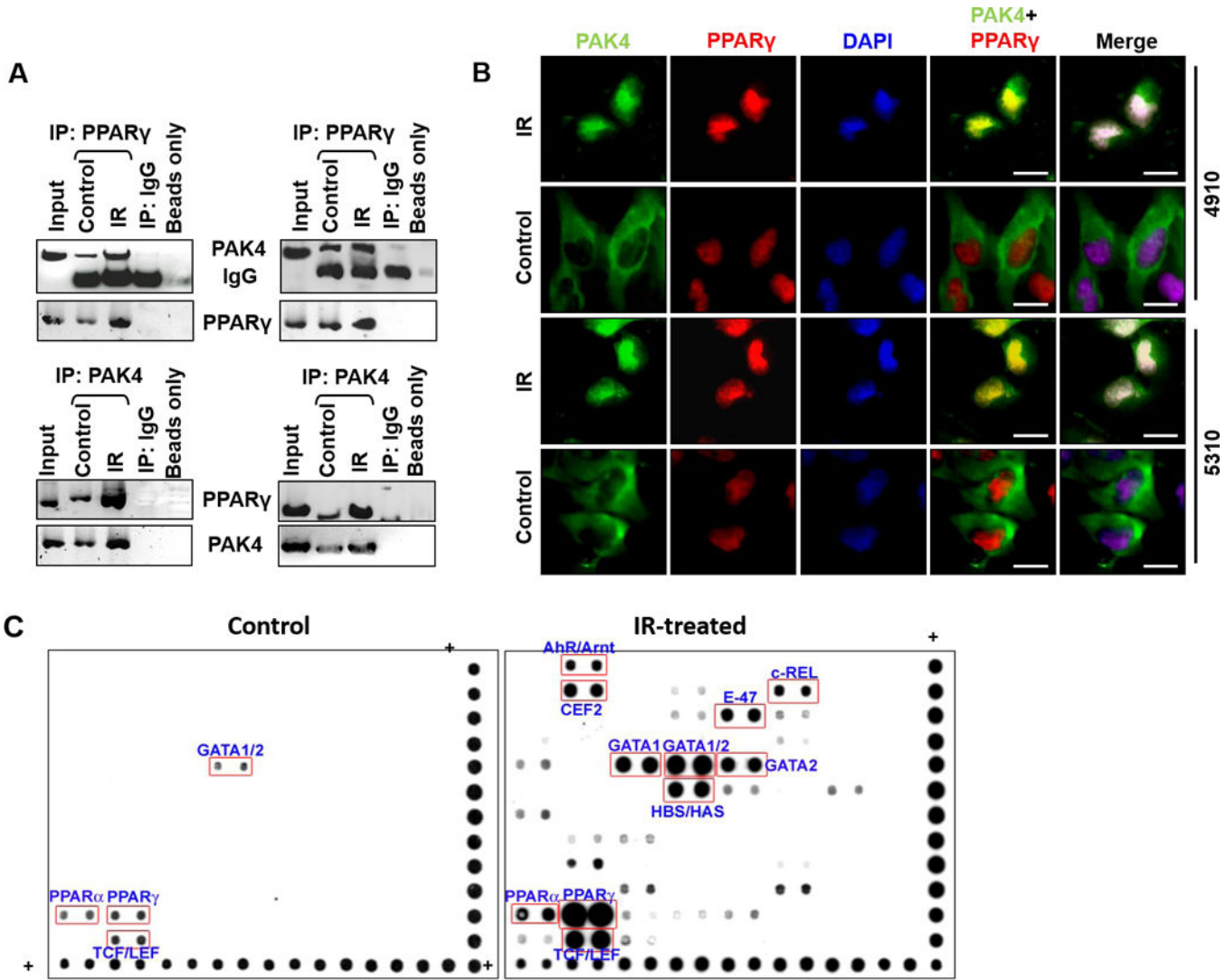


**Figure 4. Radiation enhanced PAK4/PPAR $\gamma$  binding in nucleus**

(A) IP with antibodies against non-specific IgG and PPAR $\gamma$  using nuclear lysates prepared from control and IR (8Gy)-treated 4910 and 5310 cells followed by immunoprobings with PAK4 antibody (Top panels). Reciprocal IPs were performed with anti-IgG and anti-PAK4, and subsequently immunoprobed with PPAR $\gamma$  to confirm changes in radiation-induced PAK4/PPAR $\gamma$  interaction in these cells (Bottom panels). Representative blots from three independent experiments are shown. (B) Sub-cellular localization analyses of PAK4 (green) and PPAR $\gamma$  (red) by confocal microscopy in control and IR-treated cells. Scale bars: 10 $\mu$ m. (C) Protein-DNA array (version II) interaction analysis performed with immunoprecipitated PAK4 from 4910 nuclear extracts as described in Materials and Methods. PAK4 binding with TF-consensus sequences was detected by duplicate spots on the membrane. “+” indicates positive control signal.

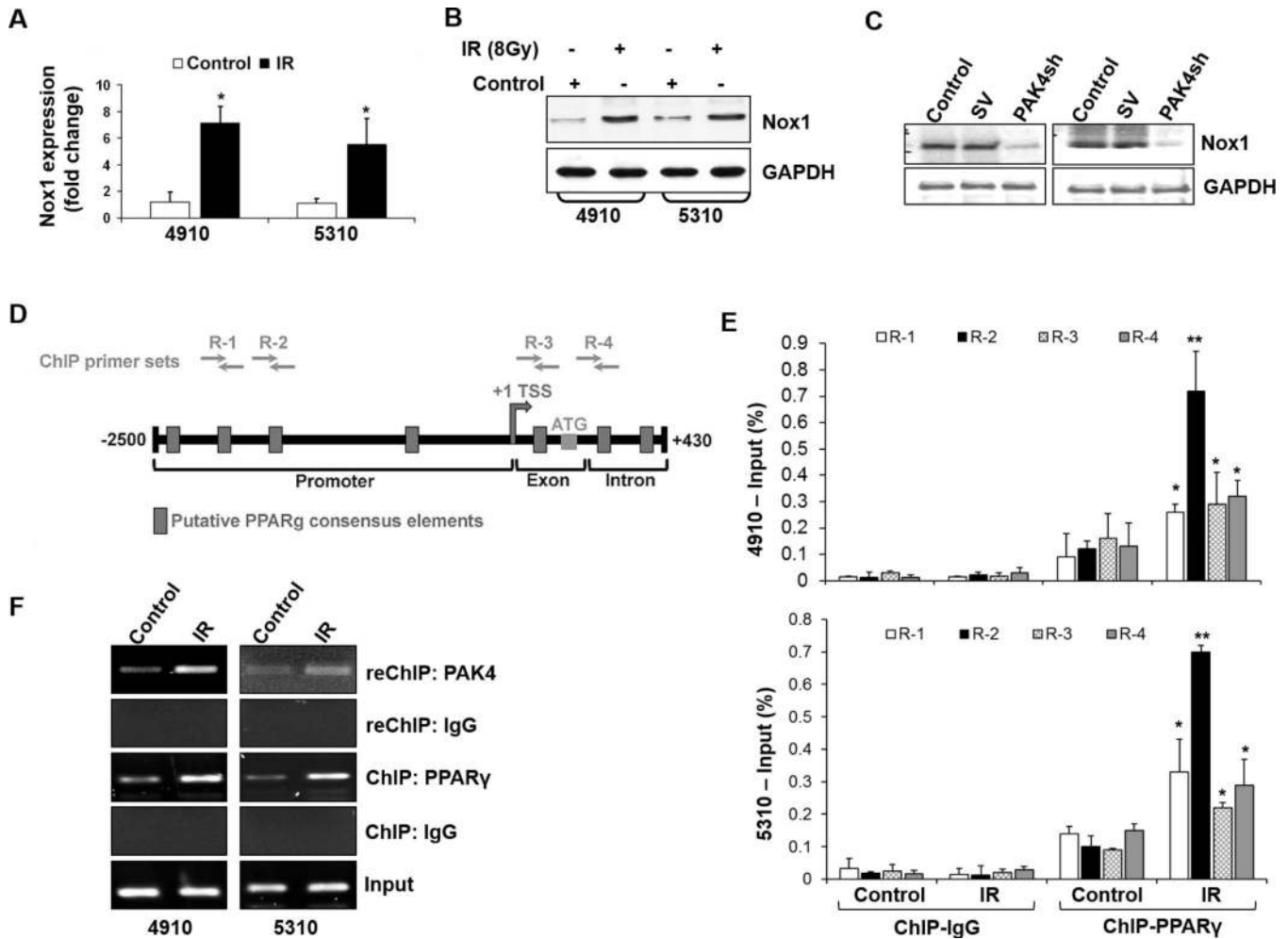


**Figure 5. Radiation-induced PAK4/PPAR $\gamma$  recruitment on the PPAR $\gamma$ -binding site on Nox1 promoter**

(A) Real-time PCR showing Nox1 transcriptional levels in control- and IR-treated cells. The fold change values are represented as mean  $\pm$  SD (n=5) obtained from at least three independent experiments (\*p  $\leq$  0.01). (B) Immunoblotting shows Nox1 expression with GAPDH served as an internal control. (C) Whole cell lysates were subjected immunoblotting and representative blots from three independent experiments were shown. (D) Schematic representation of putative PPAR $\gamma$  binding sites on Nox1 promoter. Seven putative PPRE sites were identified located in the promoter (4 sites), exon-1 (1 site) and intron-1 (2 sites) of human Nox1 based on analysis of a 2.9-kb 5'-flanking region of Nox1 (GenBank: ABC40742.1). ChIP primers specific for R-1, R-2, R-3 and R-4 regions (blue arrows) were used to determine PPAR $\gamma$  recruitment on Nox1 promoter. (E) ChIP analysis of PPAR $\gamma$  occupancy around PPREs on the Nox1 promoter using DNA from 4910 and 5310 cells and IP with anti-IgG and anti-PPAR $\gamma$  antibodies with and without IR treatment. 5% of pre-ChIP DNA samples served as input controls for each sample. ChIP-DNA from control and IR-treated cells were analyzed by quantitative PCR using ChIP-specific primers covering Nox1 promoter regions (R-1 to R-4). ChIP amplification is shown as percent input from three different experiments (n=5) (\*p  $\leq$  0.05, \*\*p  $\leq$  0.01). (F) ChIP assay was performed



with R-2 primers and antibodies against non-specific IgG and PPAR $\gamma$  using CHIP-DNA as described above in both 4910 and 5310 cells. Subsequently, re-ChIP assay was performed using primary ChIP amplicons with anti-IgG and anti-PAK4 antibodies; results from three experimental replicates are shown.

Author Manuscript

Author Manuscript

Author Manuscript

Author Manuscript

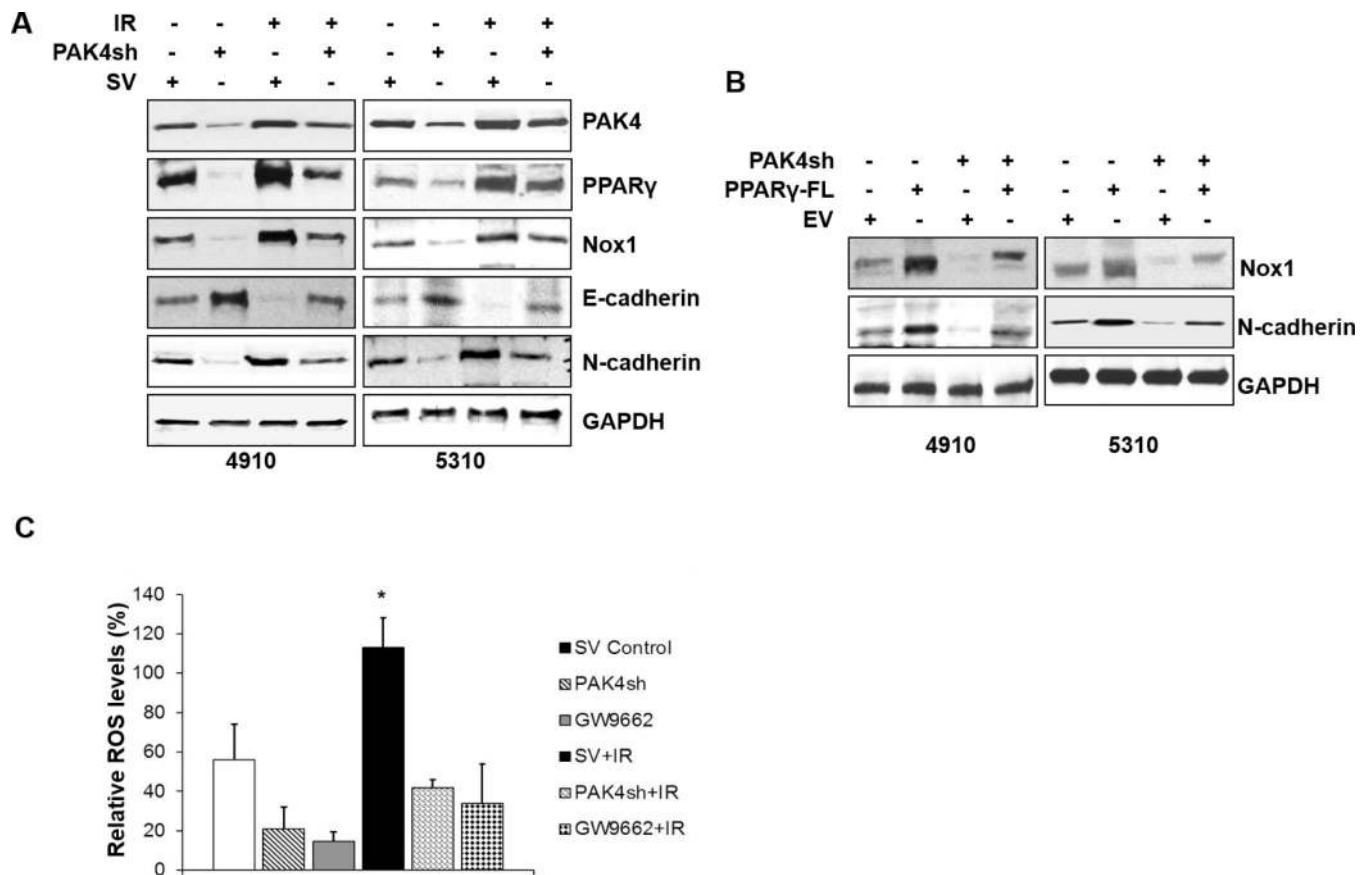


**Figure 6. Role of PAK4 in the regulation of PPAR $\gamma$ -mediated Nox1 and EMT in glioma cells** (A) Cells were subjected to SV and PAK4sh for 24 hours and subsequently treated with IR for an additional 24 hours. At the end of the treatments, whole cell lysates were subjected to western blotting with GAPDH as internal loading control. (B) Cells were treated with EV and PPAR $\gamma$ -FL for 24 hours followed by treatment with PAK4sh for an additional 24 hours. Western blotting was performed with whole cell lysates; representative blots from three independent experiments are shown. (C) 4910 cells were treated independently with SV-control or PAK4sh or GW9662 (10 $\mu$ M) or IR (8Gy) or with combinations of SV+IR, PAK4sh+IR and GW9662+IR for 48 hours. Total ROS levels were estimated as described in Materials and Methods and are presented as mean  $\pm$  SD from three experimental replicates (\* $p$   $\leq$  0.01).

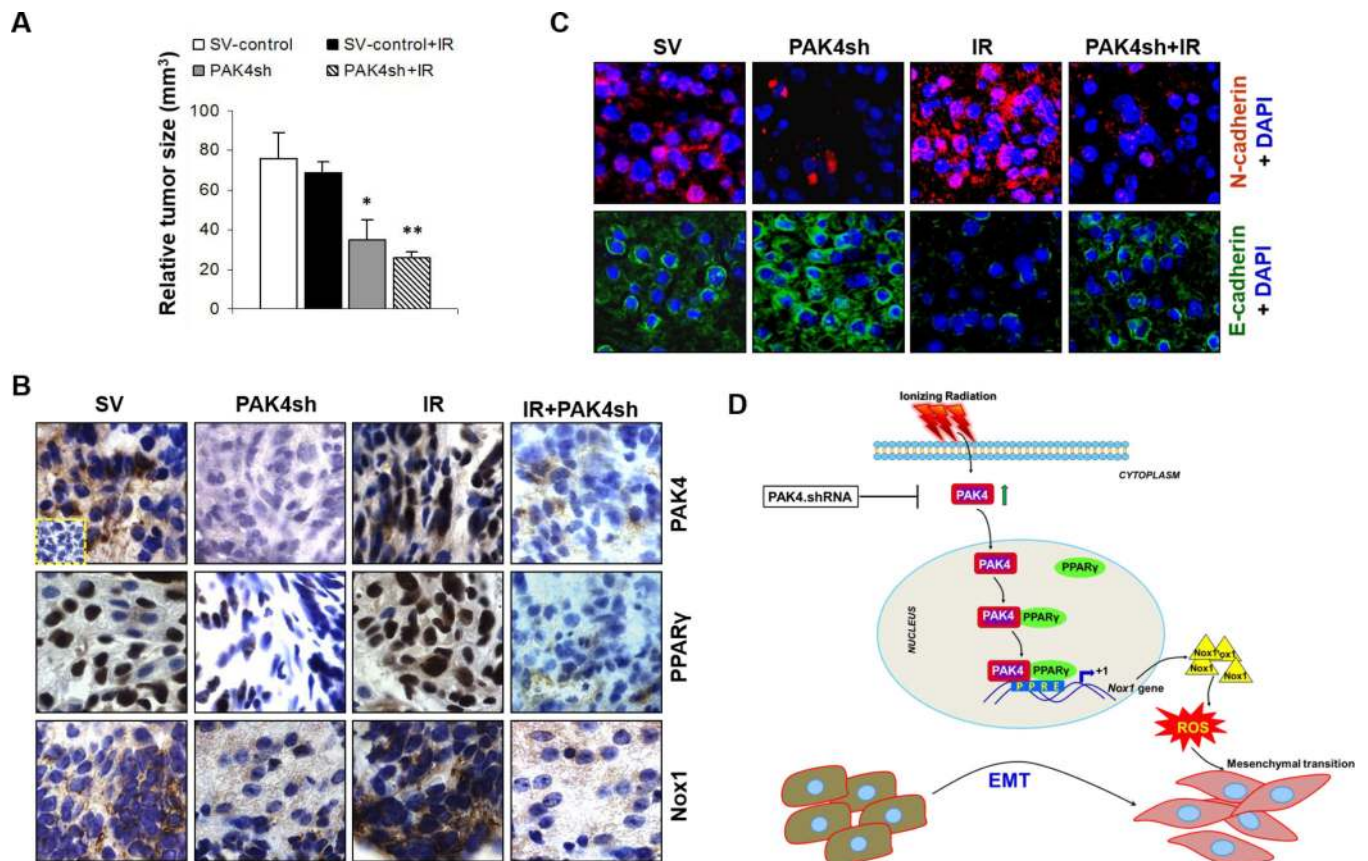


**Figure 7. Effect of PAK4 downregulation on orthotopic tumor growth in nude mice**

(A) Paraffin-embedded brain tumor sections were stained and tumor volumes were measured as described in Materials and Methods. Relative tumor size is shown as mean  $\pm$  SD obtained from different groups as indicated (n=6) (\*p  $\leq$  0.05, \*\*p  $\leq$  0.01). (B) Immunohistochemical analysis of brain tumors from nude mice that were intracranially implanted with SV or PAK4sh cells and subjected to IR treatments as described in Materials and Methods; representative micrographs are shown. Inset: staining with Non-specific IgG. (C) Confocal microscopy was performed in tumor sections to determine N-cadherin (red) and E-cadherin expression (green) levels. (D) Schematic diagram represents the radiation-induced PAK4 nuclear translocation, binding with PPAR $\gamma$  and co-recruitment of PAK4/PPAR $\gamma$  complex on to Nox1 promoter which further results in Nox1 transactivation, ROS generation and EMT induction in glioma cells.